SOLSTICE:
An Electronic Journal of Geography and Mathematics.

(Major articles are refereed; full electronic archives linked)

Congratulations to all ***Solstice*** contributors:
Solstice was a SemiFinalist (top 80 in the world out of over 1000 entries), Pirelli INTERNETional Award, 2001.

CURRENT ISSUE
SOLSTICE, VOLUME XIV, NUMBER 1;
SUMMER, 2003.

Kulwinder Kaur
On L^1-Convergence of Modified Sine Sums
TeX file link.

Sandra Lach Arlinghaus
1. Ann Arbor, Michigan: Virtual Downtown Experiments

2. Tornado Siren Location: Ann Arbor, Michigan

Special section, I, on Ann Arbor, Michigan.
In commemoration of years of town/gown cooperation, associated with students in courses taught by S. Arlinghaus, 1992-present at The University of Michigan. Thanks to the following individuals in the City of Ann Arbor who made these projects possible. They have graciously supplied maps, aerials, and wise counsel on a regular basis:

- **Merle Johnson, GIS Expert, Information Technology Services, City of Ann Arbor**
- **Karen Hart, Planning Director, Planning Department, City of Ann Arbor**
- **Wendy L. Rampson, City Planner III, Planning Department, City of Ann Arbor**
- **Coy Vaughn, City Planner III, Planning Department, City of Ann Arbor**
- **Jeff Kahan, City Planner II, Planning Department, City of Ann Arbor**
- **Chandra Hurd, City Planner II, Planning Department, City of Ann Arbor**
- **Matthew Kowalski, Assistant Planner, Planning Department, City of Ann Arbor**
- **Heather R. Edwards, Historic Preservation Coordinator, City of Ann Arbor**
- **Matthew Naud, Environmental Coordinator, City of Ann Arbor**
- **Ethel Potts, Zoning Board of Appeals**
- **Jean Carlberg, City Council**

Please e-mail if interested in files that are no longer posted; they may be available.

New Projects in Solstice, reflecting interaction between University of Michigan students (or others) and municipal authorities.	Links to existing projects already published in Solstice.	Links (and citations) to older projects, not in Solstice, reflecting interaction between University of Michigan students and municipal authorities
• **Parks and Schools Directory: Ann Arbor/Pittsfield**, Peter Z. Acuff, Winter 2003 • **Bike Parking in Downtown Ann Arbor**, Simon VanLeeuwen, Winter 2003 (use Internet Explorer). • **Urbanimals Map**, Emile Lauzzana, Winter 2003. • **Ann Arbor Historic Preservation**, Ronald Keolian, Rachel Hornstein, and Vanessa Reisin, Fall 2002 • **Clean Waters and Green Lawns, Ann Arbor Michigan**, Adam Pettinger, Alan Striegle, Brad Fuzak, and Kathryn King, Fall 2002,	• **The Relationship between Bicycle Accidents and Lanes of Travel at Downtown Ann Arbor Intersections**, Hyeyun Lee • **Maps and Decisions: Allen's Creek Floodplain, Opportunity or Disaster?** Sandra Lach Arlinghaus • **A Neighborhood Information System within Ann Arbor, Michigan.** Sandra L. Arlinghaus and Lloyd R. Phillips. • **Elements of Spatial Planning: Theory. Part I**,	• **Field Test Site: Pall Gelman Sciences** Matthew Gamache, 2002. • Parking counts for Planning Department by David Brandt and Jacob Frysinger. • **Ann Arbor Creeksheds: Resource Website**, Sandra L. Arlinghaus, 2001. • **Digital Flood Map Project: Township Island Component**, Milo Tilton, Fall 2001 • **The Ann Arbor Freeway System**, Michael Baysdell, Fall 2000. • **Fazoli Site:**

Part II. Sandra L. Arlinghaus.

Baseline Study. Jocelyn La Face, Summer 1999.

- **Surface Flow and Steep Slopes Resource Page** Sandra L. Arlinghaus, 1999.
- Rosalyn Scaff, Fall 1999. Base for current city site.
  Project funded through the City of Ann Arbor; she won a "Community Service Professional Award" for her work (along with Wendy Rampson, Chandra Hurd, and Sandra Arlinghaus). Ongoing work to update this material by Wayne Buente.
- **A History of Landscape Change in a Neighborhood of Ann Arbor**, Katya Podsiadlo, Fall 1998.
- Amie Ottinger, Fall 1997. Base for a Parks website dealing

		with prescribed burns.

Mail

Solstice Archive

1964 Boulder Drive
Ann Arbor, MI 48104

734.975.0246
image@imagenet.org

Solstice:

An Electronic Journal of Geography and Mathematics

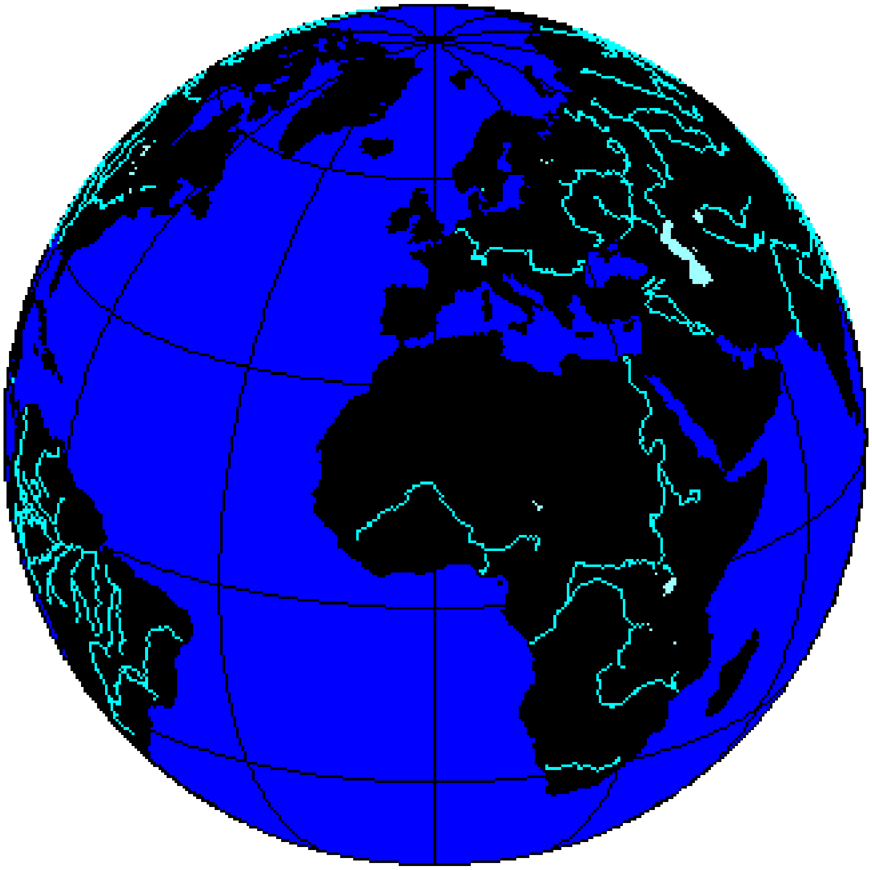

Earth: with 23.5 degrees north latitude as the central parallel.

Volume XIV
Number 1
June, 2003

Institute of Mathematical Geography (IMaGe)

SOLSTICE: AN ELECTRONIC JOURNAL OF GEOGRAPHY AND MATHEMATICS

http://www.imagenet.org

SUMMER, 2003

VOLUME XIV, NUMBER 1

ANN ARBOR, MICHIGAN

WebSite: http://www.imagenet.org

Electronic address: sarhaus@umich.edu

MISSION STATEMENT

The purpose of Solstice is to promote interaction between geography and mathematics. Articles in which elements of one discipline are used to shed light on the other are particularly sought. Also welcome are original contributions that are purely geographical or purely mathematical. These may be prefaced (by editor or author) with commentary suggesting directions that might lead toward the desired interactions.
Individuals wishing to submit articles or other material should contact an editor, or send e-mail directly to sarhaus@umich.

edu.

SOLSTICE ARCHIVES

Back issues of Solstice are available on the WebSite of the Institute of Mathematical Geography, http://www.imagenet.org and at various sites
that can be found by searching under "Solstice" on the World Wide Web. Thanks to Bruce Long (Arizona State University, Department of Mathematics)
for taking an early initiative in archiving Solstice using GOPHER.

PUBLICATION INFORMATION

The electronic files are issued yearly as copyrighted hardcopy in the Monograph Series of the Institute of Mathematical Geography. This
material will appear in a Volume in that series, ISBN to be announced.

To cite the electronic copy, note the exact time of transmission from Ann Arbor, and cite all the transmission matter as facts of publication. Any copy that
does not superimpose precisely upon the original as transmitted from Ann Arbor should be presumed to be an altered, bogus copy of *Solstice*. The
oriental rug, with errors, serves as the model for creating this weaving of words and graphics.

Recent Awards to Solstice Authors

- Jeffrey A. Nystuen, won the 2003 **Medwin Prize** in Acoustical Oceanography given by the Acoustical Society of America. The citation was "for the innovative use of sound to measure rainfall rate and type at sea". It is awarded to a young/mid-career scientist whose work demonstrates the effective use of sound in the discovery and understanding of physical and biological parameters and processes in the sea.
- Sandra L. Arlinghaus, William C. Arlinghaus, and Frank Harary. ***Graph Theory and Geography: an Interactive View (eBook)***, published by John Wiley and Sons, New York, April 2002. Finished as a **Finalist** in the 2002 Pirelli INTERNETional Award Competition (in the top 20 of over 1200 entries worldwide). Link to Pirelli website, to Pirelli award flyer, and to downloaded pages concerning this particular competition: 1, 2, 3.

IN MEMORIAM

William D. Drake
April 13, 1936-June 13, 2003.

Professor, School of Natural Resources and Environment, The University of Michigan (with affiliated appointments in the Taubman College of Architecture and Urban Planning and in the School of Public Health)

http://www-personal.umich.edu/~wddrake

Community Systems Foundation, President: http://www.CommunitySystemsFoundation.org
Archive: http://www-personal.umich.edu/~copyrght/csf/

Link to last birthday party: http://www-personal.umich.edu/~wddrake/party

---

Service to Institute of Mathematical Geography:

- Original Member, Solstice Board

- Original Member, IMaGe Monograph Board

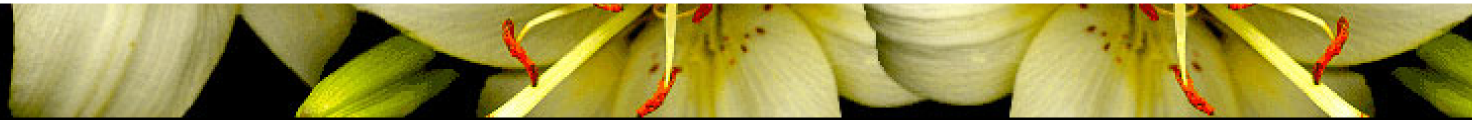

Animated Time Lines: Coordination of Spatial and Temporal Information

Sandra L. Arlinghaus, Michael Batty, and John D. Nystuen
with input from Naru Shiode*

Animation is important because it permits the portrayal of spatial information as a rapid sequence of snapshots. Thus, it integrates time with space. Many of us think of cartoons of cute animals bouncing around on a movie screen when we think of "animation." As is the case with most enduring ideas, this concept, too, has its amusing side as well as its scholarly side. Several aspects of the scholarly side have been explored in previous articles in this journal (see list of links, below), which by its internet transmission alone, lends itself as a fine medium in which to embed animations. In this paper we suggest the power of animation not only to simplify complexity, but also to coordinate sequences of information portrayed graphically.

Havlin [4] used data plots to measure differences between ranks [8] over time. He captured the differences in ranks, as a "Havlin score" on the vertical axis and the difference in time on the horizontal axis [2]. Vilensky [7] used Havlin plots to compare texts on the basis of word frequencies; books by the same author showed more in common on this factor than did books by different authors. The idea of measuring such differences is one that applies to a whole range of topics: from phase-shift diagrams, to word frequencies and authorship [7], to oil recovery [5], to agricultural applications [6], and beyond. Recently, Batty and Shiode [2] plotted populations for 459 British municipalities in Wales, Scotland, and England in 1901 by their rank differences every 10 years (Figure 1). Casual knowledge [2] suggests a British urban spatial system that is stable in form; most large cities entered the urban system by 1901. The single Havlin plot (Figure 1, Shiode created this original Havlin plot) displays a remarkably complex data set at a single glance. It also suggests the underlying stability of the dynamics of this urban system through similarity of successive pattern as one moves from left to right: color, only, serves as a guide to tracking the pattern.

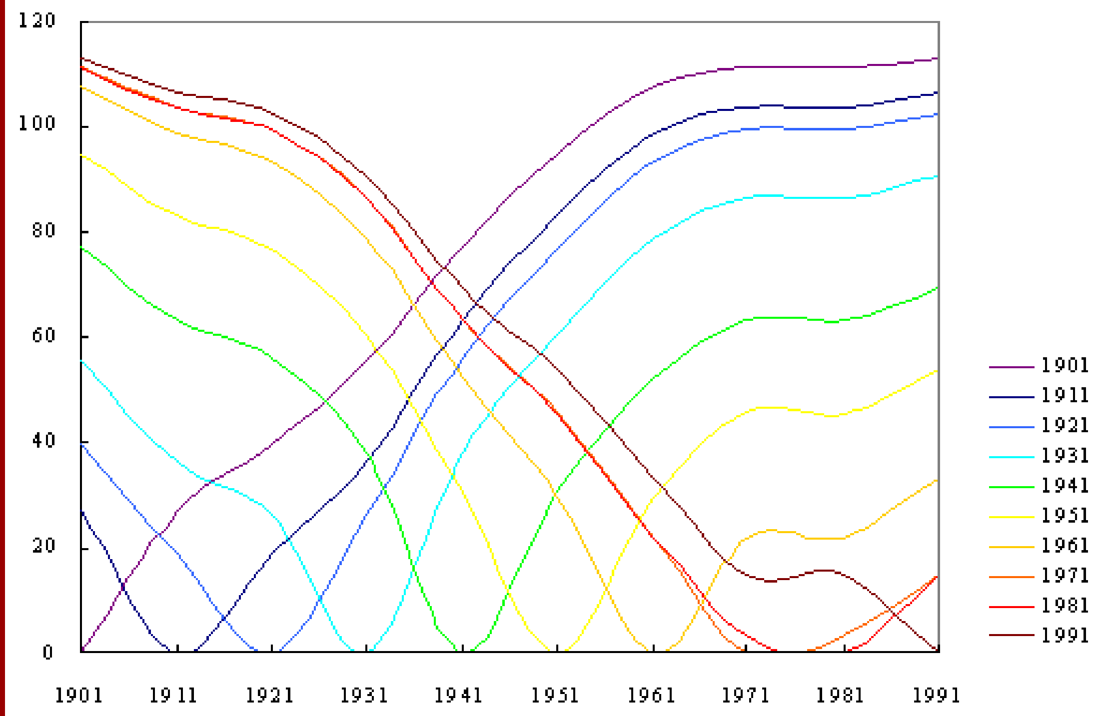

Figure 1. Static Havlin plot for rank differences in British population, 1901-1991 [2].

To gain a more focused look at this pattern, we animate the Havlin plot: a dynamic visual serves as a model for the underlying dynamic system (Figure 2). When the plot is animated, the time lines come into the picture in sequence; the corresponding sequence of dates for each time line is coordinated, using color, to enter the picture along with the curve. Coordination of sequences within a single image can underscore elements of that image's content. Figure 2 emphasizes the time at which a particular curve enters the system so that one can easily track the dynamics of the British urban spatial system through a complex data set. Note in particular that it is far easier to distinguish the 1971 curve from the 1981 curve in the animated figure than it is in the static figure.

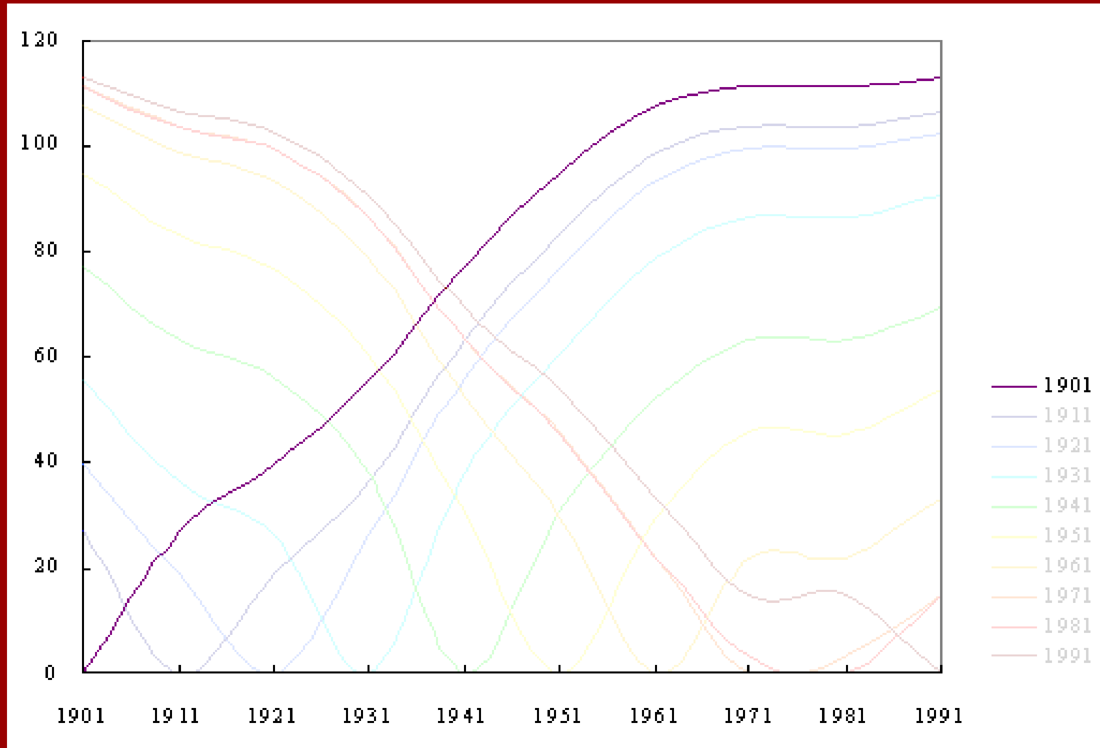

Figure 2. Animated Havlin plot coordinated with time legend.

The Havlin plot is an effective means of portraying complex urban dynamics in the British system because new cities do not enter the picture in any significant manner. If one wishes, instead, to look at a corresponding plot for United States cities, the problem of cities entering and leaving the system obscures meaning to the pattern. Thus, Batty [1] focuses instead on this entry/exit of cities from the broad urban system and expresses it in terms of half-life: the extent to which new cities enter the list of top 100 cities, at each time slice, and the extent to which cities already in this list leave the list. A plot of these values [1], tallied in a matrix, results in a somewhat inverted Havlin plot (Figure 3).

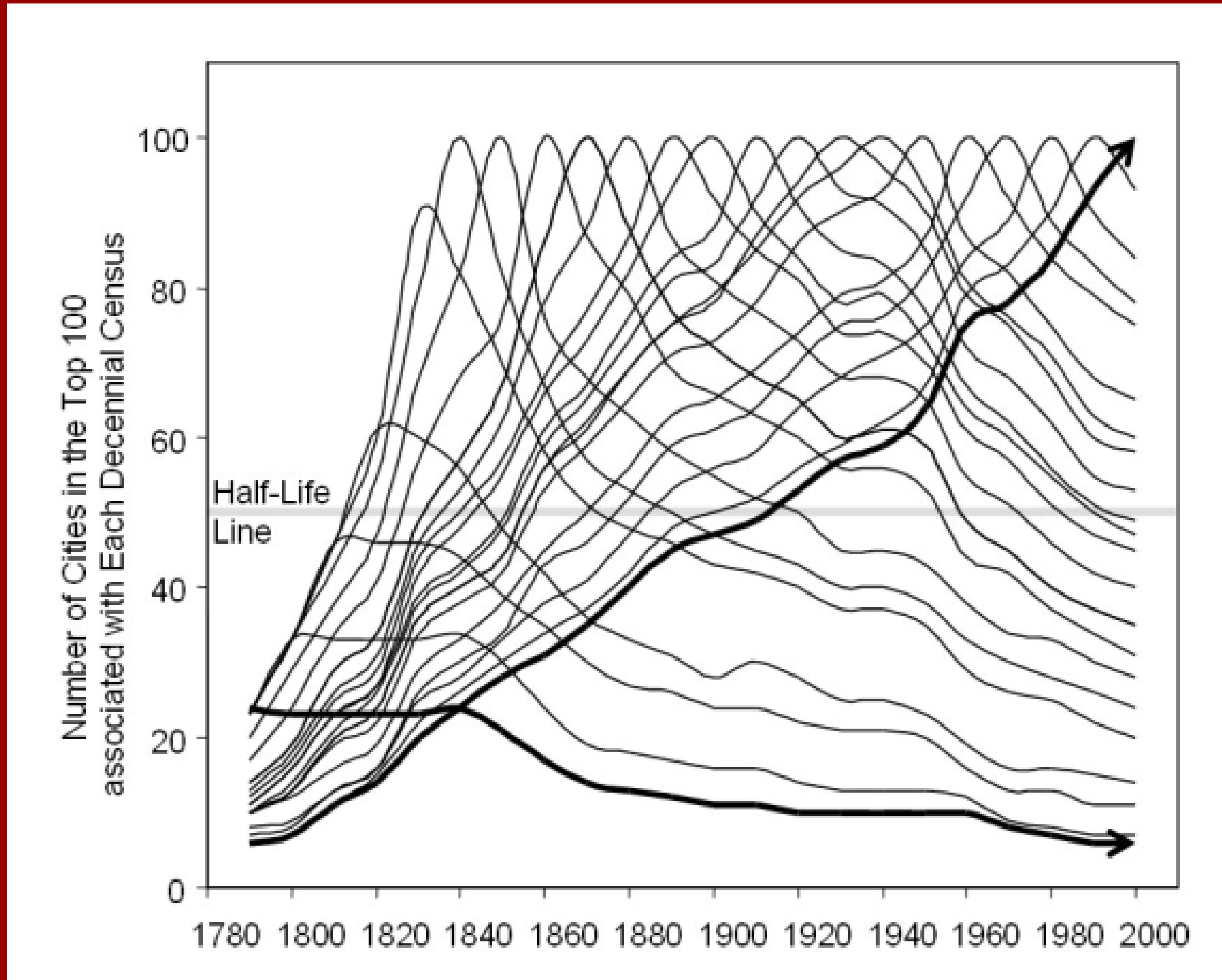

Figure 3. The Lives of US Cities from 1790 to 2000 [1].

Again, animation offers a dynamic view of a dynamic system. Time lines in Figure 4a portray an animated sequence of Figure 3: the moving blue line simplifies the otherwise complex visual pattern. The interested reader, of course, will ask about the derivation of these time lines. In conventional format, that reader might be referred to a matrix and left to run an eye up and down columns to understand the derivation of the plotted curves. Figure 4b imitates that eye movement with an animated matrix. The blue color of the curves in Figure 4a coordinates with the blue color of the matrix column outlines in Figure 4b to show clearly which column corresponds to which plotted curve: coordination of animations clarifies mathematical process. Coordination of images, each of which is itself an animated image, presents a sort of "meta" animation: an animation of animations. Thus, the transformation from the numerical to the geometric is emphasized.

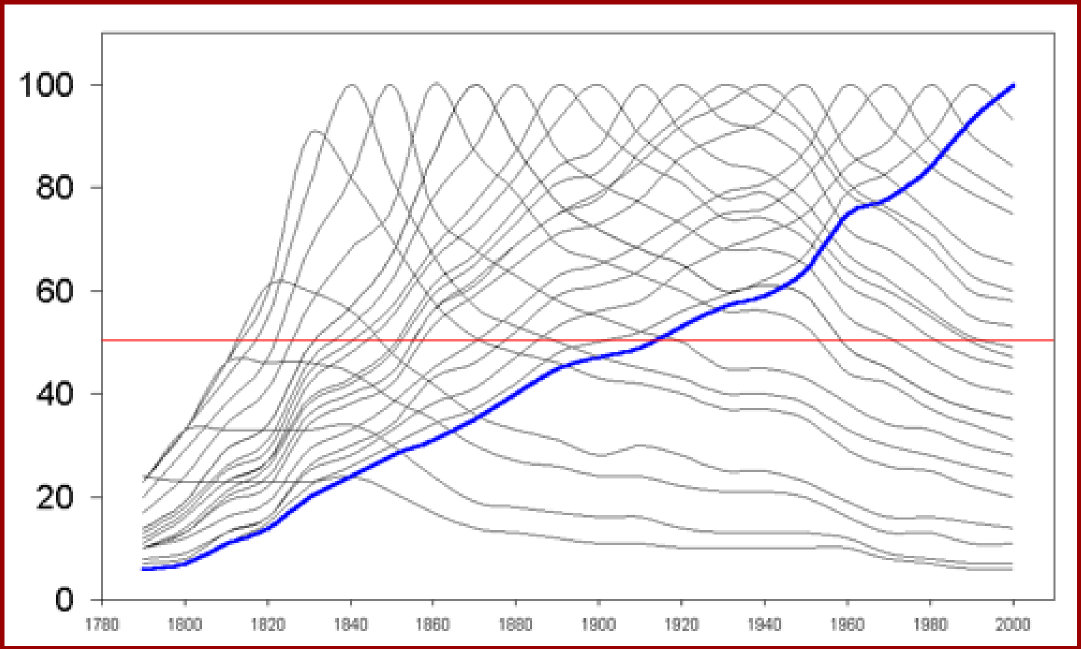

Figure 4a. Animated sequence of time lines.

	1790	1800	1810	1820	1830	1840	1850	1860	1870	1880	1890	1900	1910	1920	1930	1940	1950	1960	1970	1980	1990	2000	
1790	24	23	23	23	23	23	20	17	14	13	12	11	11	10	10	10	10	10	8	7	6	6	314
1800	23	33	33	33	33	33	29	24	19	18	17	16	16	14	13	13	13	12	9	8	7	7	423
1810	23	33	46	46	46	43	38	34	29	26	25	23	23	21	20	20	19	16	13	13	11	11	579
1820	23	33	46	61	60	55	47	41	34	31	29	27	27	26	24	24	22	19	16	16	15	14	690
1830	23	33	46	60	90	80	68	57	49	46	44	42	39	38	36	36	34	29	26	25	22	20	943
1840	24	34	44	56	82	100	82	68	57	53	50	48	43	42	40	40	38	33	30	28	26	24	1042
1850	21	30	39	48	70	82	100	76	67	62	57	55	49	48	44	44	42	38	34	33	30	28	1097
1860	17	24	35	42	58	67	76	100	86	78	68	66	61	59	56	56	53	45	43	38	34	31	1193
1870	14	19	30	36	51	57	68	87	100	88	77	73	67	65	61	62	59	50	46	41	37	35	1223
1880	13	18	27	33	48	53	63	79	88	100	87	82	76	73	69	69	65	56	52	47	42	40	1280
1890	12	17	26	31	46	50	58	69	77	87	100	93	84	81	75	75	71	63	59	53	48	45	1320
1900	11	16	24	28	43	47	55	66	72	81	92	100	88	83	78	79	73	65	61	56	50	47	1315
1910	11	16	24	30	42	45	52	63	68	77	85	90	100	92	87	85	78	69	64	58	52	49	1337
1920	10	14	22	28	40	43	50	60	65	73	81	84	91	100	94	92	86	74	70	64	56	53	1350
1930	10	13	21	25	37	40	45	56	60	68	74	78	85	93	100	96	90	79	75	68	59	57	1329
1940	10	13	21	25	37	40	45	56	61	68	74	79	83	91	96	100	93	81	76	71	62	59	1341
1950	10	13	20	23	35	38	43	53	59	65	70	73	77	85	90	93	100	87	82	75	67	64	1322
1960	10	12	16	19	29	33	38	44	49	55	61	64	67	72	79	81	87	100	92	84	79	75	1246
1970	8	9	13	16	26	30	34	42	45	51	57	60	62	68	75	76	82	92	100	89	83	78	1196
1980	7	8	13	16	25	28	33	37	40	46	51	55	56	62	68	71	75	84	89	100	90	84	1138
1990	6	7	11	15	22	26	30	34	37	42	47	50	51	55	60	63	68	79	83	90	100	93	1069
2000	6	7	11	14	20	24	28	31	35	40	45	47	49	53	58	60	65	75	78	84	93	100	1023
totals	316	425	591	708	963	1037	1102	1194	1211	1268	1303	1316	1305	1331	1333	1345	1323	1256	1206	1148	1069	1020	

Figure 4b. Animated sequence of matrix columns.

Figure 4. Animated sequence of time lines (4a) coordinated with animated sequence of matrix columns (4b) to show derivation of plotted curves.

In the current Internet climate, this technique of image coordination can be effective only if the targeted audience is known to have high speed connections to the Internet or has the capability to download and view the image on a modern computer. Otherwise, the timing between successive images quickly goes out of kilter; fortunately, however, modern computing capability is rapidly becoming more affordable and more widespread. Figure 4, viewed as a single whole, displays this sort of synthesis of animations. Dynamic images of all sorts, including coordinated sets of images that are themselves dynamic, serve as models for dynamic systems.

---

*Naru Shiode (SUNY-Buffalo) produced the data for the Havlin plots (see http://www.casa.ucl.ac.uk/naru/portfolio/

social.html)

References

1. Batty, Michael. The Emergence of Cities: Complexity and Urban Dynamics, in press, 2003.
2. Batty, Michael and Shiode, Naru. Population Growth Dynamics in Cities, Countries, and Communication Systems, in press, 2003.
3. Bunde, A. and Havlin, Shlomo [eds.] *Fractals and Disordered Systems*, 2nd ed., Springer, New York, 1996.
4. Havlin, Shlomo. The distance between Zipf plots. *Physica A* 216 (1): 148-150, 1995.
5. Lee, Youngki; Andrade, Jr., Jose S.; Buldyrev, Sergey V.; Dokholyan, Nikolay V.; Havlin, Shlomo; King, Peter R.; Paul, Gerald; and, Stanley, H. Eugene. Traveling time and Traveling Length in Critical Percolation Clusters, *Physical Review E*, Volume 60, Number 3, September 1999.
6. Stucki, J. W. and Lee, K. Improving Soil Tests for Potassium: Fundamental Considerations for Partitioning Between Fixed and Exchangeable Forms and Redox Effects, *Illinois Fertilizer Conference Proceedings*, January 25-27, 1999.
7. Vilensky, B. Can analysis of word frequency distinguish between writings of different authors? *Physica A* 231: 705-711, 1996.
8. Zipf, G. K. Human Behavior and The Principle of Least Effort, Cambridge, MA, Addison-Wesley, 1949.

Links to previous articles in *Solstice*. Back to top.

- Sandra Arlinghaus, Salma Haidar, and Mark Wilson Animated Map Timeline, Syria Volume XIII, Number 1, 2002
- Hyeyun Lee, The Relationship between Bicycle Accidents and Lanes of Travel at Downtown Ann Arbor Intersections Volume XIII, Number 1, 2002
- Jeanine Chura McCloskey, Beach Closures in Oakland County, Michigan: Using GIS as an Investigative Tool Volume XIII, Number 1, 2002
- Makoto Noguchi, The Possibility of Extending the Streetcar Line in Kagoshima City, JapanVolume XIII, Number 1, 2002
- Sandra Lach Arlinghaus,
    - The Lights Are On, All Over the World Volume XIII, Number 1, 2002
    - Base Maps, Buffers, and Bisectors Volume XII, Number 2 , 2001
    - Animaps, IV: Of Time and Place Volume XI, Number 1, 2000
- Courtney Gober, Animaps, Again
- Nakia D. Baird, Animap Sequences
- Sandra L. Arlinghaus and William C. Arlinghaus. Animaps III: Color Straws, Color Voxels, and Color Ramps Volume X, Number 1, 1999
- Sandra Lach Arlinghaus.
    - Animated Four Color Theorem: Sample Map. Volume IX, Number 2, 1998
    - Animaps, II. Volume IX, Number 2, 1998
- Sandra L. Arlinghaus, William D. Drake, and John D. Nystuen with data and other input from: Audra Laug, Kris S. Oswalt, and Diana Sammataro. Animaps. Volume IX, Number 1, 1998
- Sandra L. Arlinghaus, Ruben De la Sierra. Revitalizing Maps or Images? Volume IX, Number 1, 1998

Viewing the relative importance of some surface parameters associated with pre-monsoon thunderstorms through Ampliative Reasoning

Sutapa Chaudhuri and Surajit Chattopadhyay
Department of Atmospheric Sciences
University of Calcutta, India

Address for correspondence: 92, APC Road,Calcutta-700 009

Abstract

Instead of going into the physical detail of the pre-monsoon thunderstorms of north eastern India, a mathematical study has been done to discern the relative importance of some prominent surface parameters namely, surface temperature, relative humidity and air-pressure, in creating severe thunderstorms over the aforesaid region. The dataset associated with this weather phenomenon has been explored through the technique of Ampliative Reasoning. It has been finally found that surface temperature has the most important role in creating pre-monsoon thunderstorms. Relative humidity is less important and air-pressure is the least important.

Key words: Ampliative reasoning, Entropy, thunderstorms

Introduction:

The pre-monsoon thunderstorm, locally known as a Nor'wester, represents a mesoscale phenomenon. This kind of severe storm happens over the Northeastern part of India during the period of pre-monsoon (March-May). Since the pre-monsoon thunderstorms are generally accompanied by torrential rain, high wind speed, hail and so forth, an appropriate prediction with sufficient lead-time has continued to be a challenge to atmospheric scientists. Almost all experiments related to prediction of these storms have been based either upon statistical or numerical techniques (Murphy et al. 1989 [4], Wilks 1997 [5], Kumar et al. 1996 [3]). The complexity of the meteorological system and insufficient data has recurrently led to flawed results. Consequently, no method to date has proved sufficient to predict pre-monsoon thunderstorms over the Northeastern part of India.

The present paper uses the method of "Ampliative" reasoning (Klir and Folger, 2000) [2] to arrange, according to importance, some prominent surface parameters associated with this kind of thunderstorm. The percentage changes in the magnitudes of the corresponding parameters have been taken as the inputs for the study. Ampliative reasoning has been applied to discern the variation in the entropy associated with the probability distributions corresponding to the expected changes (%) in the magnitudes of the parameters under study. The parameter with maximum fluctuation in the entropy with change in the expected change in the magnitude (%) has been identified as the most important parameter associated with the pre-monsoon thunderstorm of the region. Surface parameters tested in this paper are: surface temperature, relative humidity, and air pressure.

Ampliative Reasoning:

Ampliative Reasoning is a probabilistic adaptation of a more general principle of reasoning in which the conclusions are not entailed in the given premises. This principle is based on two statements:

Knowing ignorance is strength.

Ignoring knowledge is sickness.

When applied within the framework of probability theory, this principle is made operational by employing Shannon entropy as the unique measure of information. Here, among all probability distributions that conform to the evidence, the chosen distribution needs to be ensured to have maximum uncertainty (i.e. minimal information) (Burg, 1967) [1]

Thus, the problem is to determine a probability distribution that maximizes the function:

$$H(p_1, p_{2,\ldots}, p_n) = -\sum_{i=1}^{n} p_i \ln p_i \quad \ldots\ldots(1)$$

The constraints are:

i) $p_i \geq 0 \forall i \in N$

ii) $\sum_{i=1}^{n} p_i = 1$

iii) $\mathrm{E}(x) = \sum_{i=1}^{n} p_i x_i$

We construct the Lagrangian,

$$L = -\sum_{i=1}^{n} p_i \ln p_i - \boldsymbol{a}\left(\sum_{i=1}^{n} p_i - 1\right) - \boldsymbol{b}\left(\sum_{i=1}^{n} p_i x_i - \mathrm{E}(x)\right) \ldots\ldots\ldots\ldots\ldots\ldots\ldots\ldots \quad (2)$$

Where $\boldsymbol{a}$ and $\boldsymbol{b}$ are Lagrange Multipliers.

Partial differentiation of equation (2) yields:

$$\frac{\partial L}{\partial p_i} = -\lambda n p_i - 1 - \boldsymbol{a} - \boldsymbol{b} x_i = 0 \ldots\ldots\ldots\ldots\ldots\ldots\ldots\ldots \quad (3)$$

$$\frac{\partial L}{\partial \boldsymbol{a}} = \quad 1 - \sum_{i=1}^{n} p_i \ldots\ldots\ldots\ldots\ldots\ldots\ldots\ldots \quad (4)$$

$$\frac{\partial L}{\partial \boldsymbol{b}} = \mathrm{E}(x) - \sum_{i=1}^{n} p_i x_i \ldots\ldots\ldots\ldots\ldots\ldots\ldots\ldots \quad (5)$$

Using (3) and i = 1,2,3,…,n

$$\left.\begin{aligned} p_1 &= \exp(-1 - \boldsymbol{a} - \boldsymbol{b} x_1) \\ p_2 &= \exp(-1 - \boldsymbol{a} - \boldsymbol{b} x_2) \\ \\ p_n &= \exp(-1 - \boldsymbol{a} - \boldsymbol{b} x_n) \end{aligned}\right\} \ldots\ldots\ldots\ldots\ldots\ldots\ldots\ldots (6)$$

So, $$p_i = \frac{\exp(-\boldsymbol{b} x_i)}{\sum_{k=1}^{n} \exp(-\boldsymbol{b} x_k)} \ldots\ldots\ldots\ldots\ldots\ldots\ldots\ldots (7)$$

Therefore, $$E(x) = \frac{\sum_{i=1}^{n} x_i \exp(-\boldsymbol{b} x_i)}{\sum_{i=1}^{n} \exp(-\boldsymbol{b} x_i)}$$

$$\Rightarrow \sum_{i=1}^{n} \left[x_i - E(x)\right] \exp(-\boldsymbol{b} x_i) = 0 \ldots\ldots\ldots\ldots\ldots\ldots\ldots\ldots (8)$$

When (8) is solved for b and the solution is substituted in (7), maximum entropy probabilities are obtained and thus, maximum H ($p_1, p_2, ..., p_h$) is achieved.

Data and Analysis:

In the present study, thunderstorms occurring over Calcutta (Kolkata), Bhubaneswar, Agartala, Gopalpur have been considered. The number of thunderstorms considered in this study is 65. Values of the previously mentioned parameters before and after thunderstorms have been taken and percentage changes in the values due to thunderstorms have been calculated.

Results, Discussion, and Conclusion:

Equation (8) has been framed by varying n from 1 to 65 for each of the parameters. The expected changes (%) in the magnitudes of the parameters have been put in the place of $E(x)$. Each equation framed this way has a ‘ b ’ that has been found by using the Newton/Raphson method. Each solution for b has produced a maximum entropy probability distribution. Using these probability distributions, entropies as defined in (1) have been calculated for each equation. The summarized results have been displayed in Table-1. From this Table it follows that maximum fluctuation in the entropy value has occurred for surface temperature and minimum fluctuation has occurred in case of air pressure. Thus, as a consequence of severe thunderstorms of the pre-monsoon season, change in the value of surface temperature is more probable than change in the value of relative humidity and air-pressure. Feedback from these parameters into thunderstorm creation therefore suggests that surface temperature has the largest contribution (of the three parameters considered) in creating new severe thunderstorms.

Expected change in the magnitude of the parameter due to thunderstorm (%)	Entropy associated with surface temperature.	Entropy associated with relative humidity.	Entropy associated with air-pressure.
5%	13.0756	10.7634	16.0172
6%	11.0832	10.3211	15.9875
7%	10.0123	9.5674	15.0011
8%	9.1745	8.9921	14.9324
9%	7.2214	7.8764	14.1352
10%	5.3124	6.9342	14.0021
11%	3.1437	5.9873	13.5683

Table-1. A tabular presentation of the entropies associated with different expected magnitudes of changes (%) in some prominent parameters due to thunderstorms.

References:

[1] Burg, J.P.1967, Maximum entropy spectral analysis, in 37th annual international meeting, Soc.of explor. *Geophysics*, Oklahoma City, OK

[2] Klir, G.J. and T.A.Folger, 2000: *Fuzzy-sets, Uncertainty and Information*. Prentice- Hall, USA.

[3] Kumar, A., M.Horeling, A. Leetama, and P. Sardeshmukh, 1996: Assessing a GCM's suitability for making seasonal predictions, *J. Climate*, **9,** pp115-129.

[4] Murphy, A., B.G.Brown, and Y.S.Chen, 1989: Diagnostic verifications and temperature forecast, *Weather and Forecasting*, **4,** pp. 485-501.

[5] Wilks, D. S., 1997: Resampling hypothesis test for autocorrelated fields, *J. Climate*, **10**, pp. 65-82.

ON L[1] –CONVERGENCE OF MODIFIED SINE SUMS

KULWINDER KAUR

Abstract. In this paper a criterion for L^1 –convergence of a new modified sine sum with semi-convex coefficients is obtained. Also a necessary and sufficient condition for L^1 –convergence of the cosine series is deduced as a corollary.

2000 Mathematics subject classification: 42A20, 42A32.

1. Introduction. Consider the cosine series

$$g(x) = \frac{a_0}{2} + \sum_{k=1}^{\infty} a_k \cos kx \tag{1.1}$$

with partial sums defined by $S_n(x) = \frac{a_0}{2} + \sum_{k=1}^{n} a_k \cos kx$

and

let $g(x) = \lim_{n\to\infty} S_n(x)$.

Concerning the L^1-convergence of cosine series (1. 1) Kolmogorov [5] proved the following theorem:

Theorem A. *If $\{a_n\}$ is a quasi-convex null sequence, then for the L^1-convergence of the cosine series (1.1) it is necessary and sufficient that* $\lim_{n\to\infty} a_n \log n = 0$.

The case in which the sequence $\{a_n\}$ is convex, of this theorem was established by Young [9]. That is why, sometimes, this Theorem A is known as Young-Kolmogorov Theorem.

Definition[4]. A sequence $\{a_n\}$ is said to be semi-convex if $a_n \to 0$ as $n \to \infty$, and

$$(1.2) \qquad \sum_{n=1}^{\infty} n|\Delta^2 a_{n-1} + \Delta^2 a_n| < \infty, \qquad (a_0 = 0)$$

where

$$\triangle^2 a_n = \triangle a_n - \triangle a_{n+1}$$

It may be remarked here that every quasi-convex null sequence is semi- convex.

Bala R. and Ram B. [1] have proved that Theorem A holds true for cosine series with semi-convex null coefficients in the following form:

Theorem B. *If $\{a_k\}$ is a semi–convex null sequence, then for the convergence of the cosine series* (1.1) *in the metric space L, it is necessary and sufficient that* $a_{k-1}\log k = o(1)$, $k \to \infty$.

Garret and Stanojevic [2] have introduced modified cosine sums

$$g_n(x) = \frac{1}{2}\sum_{k=0}^{n}\triangle a_k + \sum_{k=1}^{n}\sum_{j=k}^{n}(\triangle a_j)\cos kx$$

Garret and Stanojevic [3], Ram [7] and Singh and Sharma [8] studied the L^1-convergence of this cosine sum under different sets of conditions on the coefficients a_n.

Later on, Kumari and Ram [6], introduced new modified cosine and sine sums as

$$f_n(x) = \frac{a_0}{2} + \sum_{k=1}^{n}\sum_{j=k}^{n}\triangle(\frac{a_j}{j})k\cos kx$$

and

$$g_n(x) = \sum_{k=1}^{n}\sum_{j=k}^{n}\triangle(\frac{a_j}{j})k\sin kx$$

and have studied their L^1- convergence under the condition that the coefficients a_n belong to different classes of sequences. Also they deduced some results about L^1-convergence of cosine and sine series as corollaries.

We introduce here new modified sine sums as

$$K_n(x) = \frac{1}{2\sin x}\sum_{k=1}^{n}\sum_{j=k}^{n}(\Delta a_{j-1} - \Delta a_{j+1})\sin kx.$$

The aim of this paper is to study the L^1 –convergence of this modified sine sum with semi-convex coefficients and to obtain the above mentioned result of Bala R. and Ram B. as a corollary.

2. Main Result. The main result is the following theorem:

Theorem 2.1. *Let $\{a_n\}$ be the semi-convex null sequence, then $K_n(x)$ converges to $g(x)$ in L^1-norm.*

Proof. We have

$$\begin{aligned} S_n(x) &= \frac{a_0}{2} + \sum_{k=1}^{n} a_k \cos kx \\ &= \frac{1}{2\sin x} \sum_{k=1}^{n} a_k \cos kx 2 \sin x \\ &= \frac{1}{2\sin x} \sum_{k=1}^{n} a_k [\sin(k+1)x - \sin(k-1)x] \\ &= \frac{1}{2\sin x} \sum_{k=1}^{n} (a_{k-1} - a_{k+1}) \sin kx + a_{n+1} \frac{\sin nx}{2\sin x} + a_n \frac{\sin(n+1)x}{2\sin x} \\ &= \frac{1}{2\sin x} \sum_{k=1}^{n} (\Delta a_k + \Delta a_{k-1}) \sin kx + a_{n+1} \frac{\sin nx}{2\sin x} + a_n \frac{\sin(n+1)x}{2\sin x} \end{aligned}$$

Applying Abel's transformation, we have

$$\begin{aligned} S_n(x) &= \frac{1}{2\sin x} \left(\sum_{k=1}^{n} (\Delta^2 a_k + \Delta^2 a_{k+1}) \tilde{D}_k(x) + (a_n - a_{n+2}) \tilde{D}_n(x) \right) \\ &\quad + a_{n+1} \frac{\sin nx}{2\sin x} + a_n \frac{\sin(n+1)x}{2\sin x}. \end{aligned}$$

Thus

$$g(x) = \lim_{n\to\infty} S_n(x)$$

$$= \frac{1}{2\sin x}\sum_{k=1}^{\infty}(\Delta^2 a_k + \Delta^2 \Delta a_{k-1})\tilde{D}_k(x)$$

Also

$$K_n(x) = \frac{1}{2\sin x}\sum_{k=1}^{n}\sum_{j=k}^{n}(\Delta a_{j-1} - \Delta a_{j+1})\sin kx.$$

$$= \frac{1}{2\sin x}\left(\sum_{k=1}^{n}(a_{k-1} - a_{k+1})\sin kx - (a_n - a_{n+2})\tilde{D}_n(x)\right)$$

Applying Abel's transformation, we have

$$K_n(x) = \frac{1}{2\sin x}\sum_{k=1}^{n}(\Delta a_{k-1} - \Delta a_{k+1})\tilde{D}_k(x)$$

$$= \frac{1}{2\sin x}\sum_{k=1}^{n}(\Delta^2 a_k + \Delta^2 a_{k-1})\tilde{D}_k(x)$$

and

$$g(x) - K_n(x) = \frac{1}{2\sin x}\sum_{k=n+1}^{\infty}(\Delta^2 a_k + \Delta^2 a_{k-1})\tilde{D}_k(x)$$

$$= \lim_{m\to\infty}\left(\frac{1}{2\sin x}\sum_{k=n+1}^{m}(\Delta^2 a_k + \Delta^2 a_{k-1})\tilde{D}_k(x)\right)$$

Thus, we have

$$\int_{-\pi}^{\pi}|g(x) - K_n(x)|dx = O(\sum_{k=n+1}^{\infty} k|(\Delta^2 a_k + \Delta^2 a_{k-1})|)$$

$$= o(1), \text{by } (1.2).$$

This proves Theorem 2.1.

Corollary. *If* $\{a_n\}$ *be the semi-convex null sequence, then the necessary and sufficient condition for* L^1*-convergence of the cosine series* (1.1) *is* $\lim_{n\to\infty} a_n \log n = 0$.

Proof. We have

$$\|S_n(x) - g(x)\| \le \|S_n(x) - K_n(x)\| + \|K_n(x) - g(x)\|$$

$$= \|K_n(x) - g(x)\|$$

$$+ \left\|(a_n - a_{n+2})\frac{\tilde{D}_n(x)}{2\sin x} + a_{n+1}\frac{\sin nx}{2\sin x} + a_n\frac{\sin(n+1)x}{2\sin x}\right\|$$

Also

$$\left\| (a_n - a_{n+2}) \frac{D_n(x)}{2\sin x} + a_{n+1} \frac{\sin nx}{2\sin x} + a_n \frac{\sin(n+1)x}{2\sin x} \right\|$$
$$= \|K_n(x) - S_n(x)\|$$
$$\leq \|K_n(x) - g(x)\| + \|S_n(x) - g(x)\|,$$

and

$$|(a_n - a_{n+2})| = \left|\sum_{k=n}^{\infty}(\Delta a_k - \Delta a_{k+2})\right|$$
$$= \left|\sum_{k=n+1}^{\infty} \frac{k}{k}(\Delta a_{k-1} - \Delta a_{k+1})\right|$$
$$\leq \frac{1}{n}\left|\sum_{k=n+1}^{\infty} k(\Delta^2 a_k + \Delta^2 a_{k-1})\right|$$

$$= o\left(\frac{1}{n}\right).$$

Since $\int_{-\pi}^{\pi} \frac{\tilde{D}_n(x)}{2\sin x}dx = O(n)$

Therefore

$$(a_n - a_{n+2}) \int_{-\pi}^{\pi} \frac{\tilde{D}_n(x)}{2\sin x}dx$$

$$= O((a_n - a_{n+2})n),$$

$$= o(1).$$

Moreover,

$$\int_{-\pi}^{\pi} \left| a_{n+1} \frac{\sin nx}{2\sin x} + a_n \frac{\sin(n+1)x}{2\sin x} \right| dx$$

$$\leq \int_{-\pi}^{\pi} a_n \left| \frac{\sin nx}{2\sin x} + \frac{\sin(n+1)x}{2\sin x} \right| dx$$

$$= a_n \int_{-\pi}^{\pi} |D_n(x)| dx$$

$$\sim (a_n \log n).$$

Since $\|K_n(x) - g(x)\| = o(1), \qquad (n \to \infty)$. by Theorem 2.1

Therefore it follows that

$$\lim_{n\to\infty} \int_{-\pi}^{\pi} |g(x) - S_n(x)| dx = o(1),$$

if and only if $\lim_{n\to\infty} a_n \log n = 0$.

REFERENCES

1. Bala R. and Ram B., Trigonometric series with semi-convex coefficients, Tamkang J. Math. 18(1)(1987), 75-84.

2. Garrett J.W. and Stanojević Č.V., On Integrability and L^1 – convergence of certain cosine sums, Notices, Amer. Math Soc. 22(1975) A-166.

3. Garrett J.W. and Stanojević Č.V, On L^1- convergence of certain cosine sums, Proc. Amer. Math. Soc. 54(1976), 101-105.

4. Kano T., Coefficients of some trigonometric series, Jour. Fac. Sci. Shihshu University 3 (1968), 153-162.

5. Kolmogorov A.N., Sur l'ordere de grandeur des coefficients de la series de Fourier – Lebesque, Bull. Polon. Sci. Ser. Sci. Math. Astronom. Phys. (1923) 83-86

6. Kumari Suresh and Ram Babu, L^1-convergence modified cosine sum , Indian J. pure appl. Math.19 (11)(1988), 1101-1104.

7. Ram B.,. Convergence of certain cosine sums in the metric space L, Proc. Amer. Math. Soc. 66(1977), 258-260.

8. Singh N. and Sharma K.M., Convergence of certain cosine sums in the metric space L, Proc. Amer. Math. Soc. 75(1978), 117-120.

9. Young W.H., On the Fourier series of bounded functions, Proc. London Math. Soc. 12(2)(1913), 41-70.

10. Zygmund A., Trigonometric Series, Vol. 1, Cambridge University Press, Cambridge, 1959.

Ann Arbor, Michigan:
Virtual Downtown Experiments

Sandra Lach Arlinghaus
The University of Michigan
with input in varying degrees from the individuals noted at the end of this article.
sarhaus@umich.edu
http://www-personal.umich.edu/~copyrght

The problem of where to locate tall buildings, with sensitivity to existing building types on adjacent and nearby lots, is a difficult one. In Ann Arbor, building height is currently limited by "floor area ratio" (FAR). The FAR is calculated as the ratio of floor area in a building divided by parcel area, times 100. If a given parcel has an FAR of 100, then a building footprint built lot line to lot line may have a height of 1 story. If a parcel has an FAR of 200, then a building footprint built lot line to lot line may have a height of 2 stories. Similarly, an FAR of 300 yields a building of height 3 stories covering the entire parcel. Thus, on a parcel with an FAR of 300, one might, instead, build a building on half of the lot area but of height six stories, or on a third of the lot area but of height 9 stories. On the same parcel, a 30 story building could be built only if its footprint covered one-tenth of the land area of the parcel. The FAR provides a height limit based on the size of foundation needed to support a tall building. It also offers subtle encouragement for preserving some amount of open space and visual variation in the region to which it applies. The drawback is that a tall building may get built with no regard to the broader context of how a new building will fit in with existing buildings on the surrounding parcels. A possible side effect of using FAR (alone) to limit height is that it might encourage parcel amalgamation by large developers, thereby driving out desired local small business owners. [Note: in Ann Arbor, there are also "premiums" designed to encourage residential construction, and other uses viewed as "desirable" in the downtown; these allow an increase in FAR. They will not be covered in this abstract discussion.]

The FAR is assigned by zoning type. In the downtown, there are currently parcels assigned to each of 22 different zoning categories (AG, C1, C1A, C1AR, C2A, C2AR, C2B, C2BR, C3, M1, M1A, M2, O, P, PL, PUD, R1D, R2A, R2B, R4B, R4C, R4D). Roughly speaking, any category beginning with C is a commercial category; M is for manufacturing; R is for residential. The AG category is for agricultural zoning, O is for office, P (except for PUD) is for Public Land (as for the University of Michigan which, as a State university, contributes no funds to the city taxpayer economic base), and PUD is for Planned Unit Development. In Figure 1, the animated map shows the City of Ann Arbor parcel map colored as a thematic map by zoning category: the broad PL zoning is part of the central campus of the University of Michigan. The curved line near the left side of the map. representing the Ann Arbor Railroad corridor, has most of the manufacturing parcels adjacent to it. Separate categories enter the picture in sequence, arranged according to alphabetical ordering of zoning category. The coloring scheme is exhaustive: every parcel is covered. It is also mutually exclusive: no parcel has more than one color. Thus, the zoning classification serves as a geometric partition of the parcels.

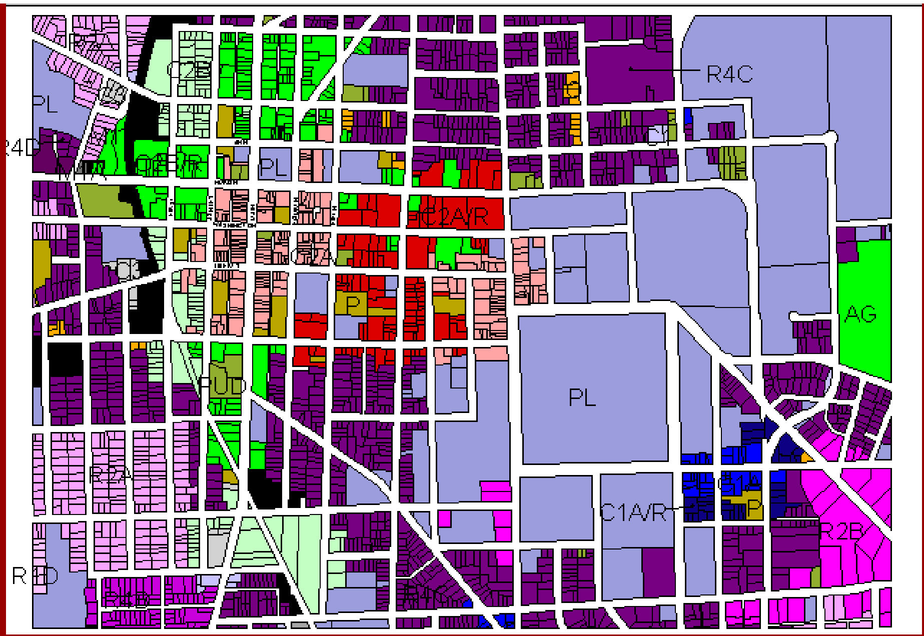

Figure 1. Zoning animation of 22 zoning categories:
AG, C1, C1A, C1AR, C2A, C2AR, C2B, C2BR, C3, M1, M1A, M2, O, P, PL, PUD, R1D, R2A, R2B, R4B, R4C, R4D. Zones enter the animation in alphabetical succession. Attached labels are added in the final frame.

Once an inventory of parcel categories is obtained by creating thematic maps, the groups of parcels will be removed in accordance with various ideas. The goal is to select targets of opportunity for taller projects as illustrated below.

Animated maps are useful for showing change; static maps are useful when one wishes to take a longer look at pattern without regard to change in pattern. Thus, Figure 2 shows the final frame of the animated map in Figure 1 along with a layer showing the boundary of the Downtown Development Authority (DDA) in yellow, the railline in black/yellow, the floodway (channel) outline of Allen's Creek in blue, and the floodplain outline of Allen's Creek in cyan.

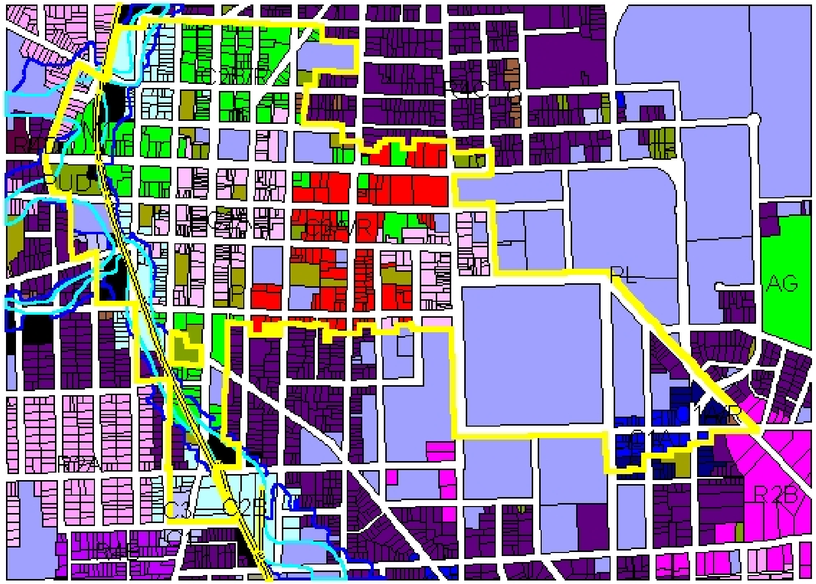

Figure 2. Zoning categories, DDA boundary, railline, floodway and floodplain.

The current interest is to consider only zoning categories, as the downtown "core," of C1A, C1AR, C2A, C2AR, C2BR as those containing parcels that are targets of opportunity for building structures of height greater than that permitted by FAR. The current FAR in these categories is either 200 or 300. The idea is that there may well be parcels within these core downtown areas that could support height in excess of that permitted by the FAR. In Figure 3, the shading is removed for these zoning categories; they are easily focused on as a grouping. When parcels containing historic district designation (and relatively short buildings) are superimposed on the pattern in Figure 3, further limitation of targets of opportunity is the result (Figure 4). The historic district parcels were inserted in a separate step because they overlap the standard zoning hierarchy and are not a part of the geometric partition noted above.

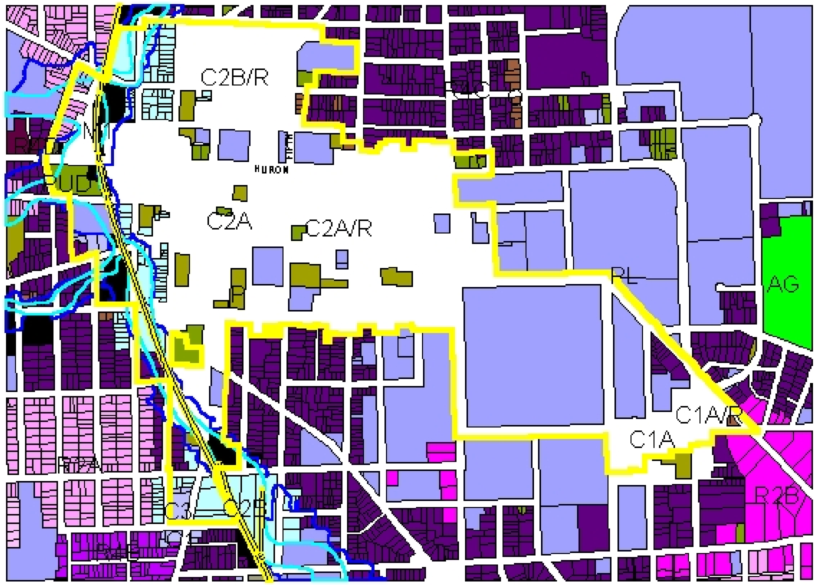

Figure 3. Shading is removed from C1A, C1AR, C2A, C2AR, C2BR zoning categories--the downtown core--to visually group these regions as those containing parcels that are targets of opportunity for height in excess of that permitted by the FAR.

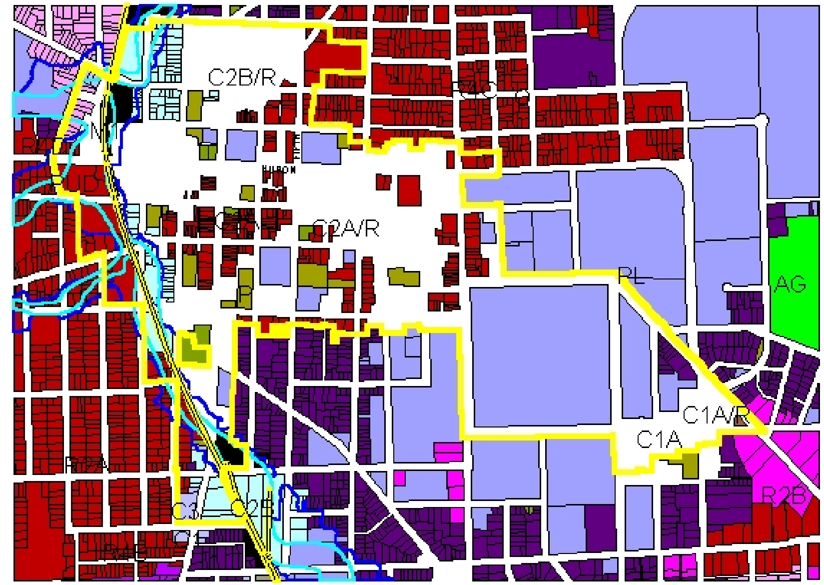

Figure 4. This map is identical to the map in Figure 3 with historic district parcels superimposed in red. The historic district designation further limits the targets of opportunity.

The white areas of the map in Figure 4 contain all the possible parcels in the downtown core that do not carry historic district designation. Some of them already have buildings built on them; others do not. Those with buildings on them may become eventual redevelopment targets; those with no buildings on them may be short-range targets. To take a closer look at the area, insert an aerial photo of the DDA behind the map in Figure 4 (as well as other items of possible interest, such as contours to identify steep slopes). Figure 5 shows a zoom-in on part of the white area; in that figure, however, the "white" area has been replaced with aerial so that one can see directly the current content of all parcels in the core that do not have historic district designation. One can see what is on each parcel and might determine, therefore, a strategy for targeting opportunities for development in excess of the FAR.

A current suggestion by the Planning Department staff and the Ordinance Revisions Committee is to use the street hierarchy to select general target areas: wider streets support taller nearby structures. Thus, the zoom-in of Figure 5 is on Huron Street, the widest street in the DDA. Use of the aerial not only permits quick determination of where parking lots and existing buildings are located but it also shows shadow pattern of existing buildings suggesting guidelines for upper story setbacks and other tools that limit reduction of light. Light in the streetscape is pedestrian-friendly (and vegetation-friendly), particularly at this mid-continental latitude. Highest priority immediate targets of opportunity for height in excess of that permitted by the FAR thus appear (from the abstract representation in Figure 5 alone) to be in the large parking lots visible along Huron Street, with suitable upper level setbacks to minimize shadow in the street. Further analysis is needed, however, to include steep slopes, opinion from members of the public and from developers, the will of governing bodies, and various other acadmic and non-academic factors.

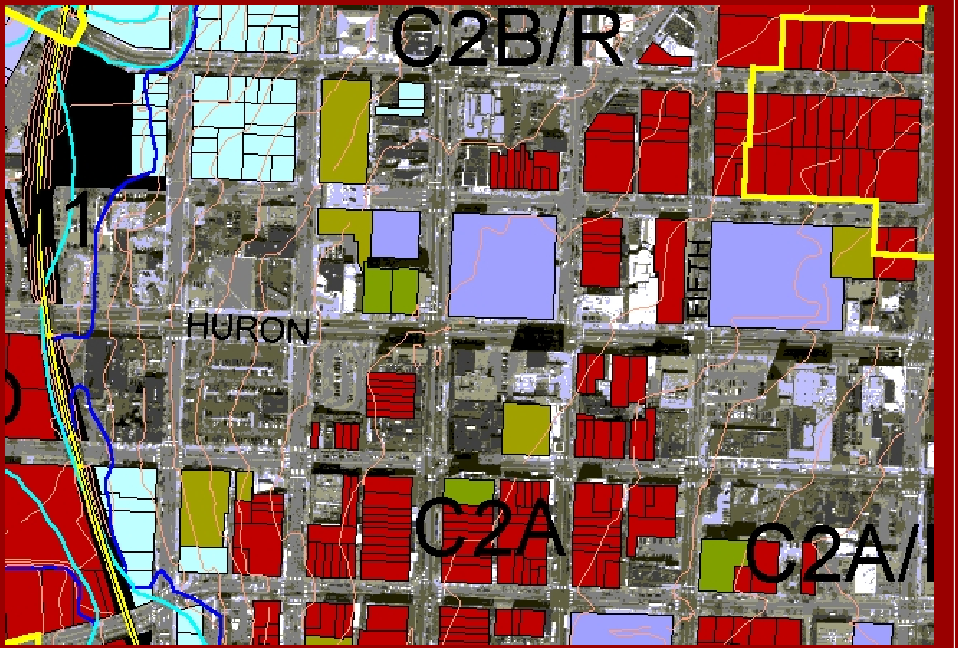

Figure 5. Zoom in--use the street hierarchy to suggest locales--notice the shadows leaning out into Huron Street as well as the content of the core area along Huron Street, from tall buildings to parking lots.

Dynamic maps, produced in Geographic Information Systems (GIS) software, when coupled with high quality aerial photography produces powerful visualization capability that can guide decision-makers. One limitation of this visual analysis is dimensional: even though the aerials are high quality, one still really has only a two-dimensional view of a three-dimensional scene. The ideal would be to have dynamic three dimensional models of the core area. Virtual reality (VR) affords such an opportunity in two different ways: through web-based virtual reality and through immersion in a virtual reality CAVE. Only the former technique can be displayed in this article. The plan, beyond the VR experiments in this article, is to take files such as these, place them in the CAVE in the Media Union at The University of Michigan North Campus in Ann Arbor, and invite policy makers to immerse themselves in the virtual reality created by alternative height scenarios (report to come in a subsequent issue of Solstice) in order to consider the issue of a maximum height ordinance or any other zoning issues in the downtown.

To view the VR experiments below (Figure 6), first download Cosmo Player and install it in your browser according to directions. Then, click on the links below and practice navigating through the streets of downtown Ann Arbor.

FAR Virtual Reality: translucent buildings are superimposed, lot line to lot line on parcels in the downtown core zones. This VR experiment depicts the downtown with the simplest use of the FAR. [The DDA region is shown in black; the Allen Creek floodplain in blue.]

Actual height Virtual Reality: again, buildings are superimposed, lot line to lot line, on parcels in the downtown core zones. This VR experiment depicts the downtown using actual building heights, where known. [The DDA region is shown in gray; the Allen Creek flooplain and floodway in shades of blue; building color is according to height category.]

Figure 6. Virtual Reality experiments performed using ArcView GIS, v. 3.2, with Spatial Analyst Extension and 3D Analyst extension (from ESRI)..

The title of this article contains the word "experiment." There remain many directions one might move from these initial experiments in order to use maps, aerials, and virtual reality as a guide to decisions. Some of these next steps are enumerated below.

- Digitize the aerial photograph of the DDA so that VR can be constructed on actual building footprints rather than only on a parcel outline basis.
- Field-check building height measurements.
- Introduce final files into an immersion CAVE environment and invite policy-makers to immerse themselves in various 3D alternatives for height in the downtown.
- Consider other patterns for zoning in the downtown. For example, one might begin with the historic district designations and buffer these with fringe areas of various heights supporting gradually increasing heights away from historic buildings (as constrained by a number of variables such as with road width or street hierarchy, proximity to residential zoning, steep slopes, design standards, or various other factors). Thus, a new geometric partition of parcels, based on historic designation, would emerge.
- Recommendation and implementation of any policy for limiting height in the downtown is beyond the scope of any of this material.

The author acknowledges productive meetings with and assistance from

- her colleagues on the City of Ann Arbor Planning Commission (Sandra Arlinghaus (Chair), Kevin McDonald (Vice-Chair), Scott Wade (Secretary), Braxton Blake, Jean Carlberg, Kristen Gibbs, Christopher Graham, William Hanson, and Steve Thorp);
- the Ordinance Revisions Committee of that Commission (Hanson, Chair; Carlberg, Arlinghaus, Blake);
- the City of Ann Arbor Planning Department staff (Karen Hart, Planning Director; Wendy Rampson, Coy Vaughn, Donna Johnson, Jeff Kahan, Chandra Hurd, Alexis Marcarello, Chris Cheng, and Matt Kowalski);
- Merle Johnson, City of Ann Arbor, Information Technology Services;
- Heather Edwards, Historic District Preservation Coordinator, City of Ann Arbor; and,
- the Mayor of Ann Arbor, His Honor, John Hieftje.

Software used: ArcView GIS, v. 3.2, with Spatial Analyst Extension and 3D Analyst Extension. All from ESRI (Environmental Systems Research Institute, Redlands, CA).

Tornado Siren Location
Ann Arbor, Michigan

Sandra Lach Arlinghaus
The University of Michigan
with input from those noted below.
sarhaus@umich.edu
http://www-personal.umich.edu/~copyrght

Different strategies for locating systems of sirens exist in different locales across the nation. In Ann Arbor, and elsewhere, sirens noise is designed to alert citizens in the outdoors. Citizens who are indoors may hear the sirens but the requirement is that people outdoors be able to hear them. Thus, spacing requirements between sirens becomes important. When there are barriers to overcome (all else being equal), such as topography, buildings and street noise, one might expect sirens to be required to be more closely spaced than in flat, open countryside. Indeed, a brief review of municipal requirements on the world wide web reveals that Oakland County, Michigan views each siren to be capable of covering about a one mile radius. The Baltimore City Fire Department selects spacing at 3200 feet.

The sequence of animaps below, of Ann Arbor, suggests a locational strategy for pinpointing positions for new sirens.

In this first animated map, Figure 1,

- the red dots show the location of the existing system of sirens.
- The light green circles are buffers of radius 3200 feet, the Baltimore standard. Employing the Baltimore standard provides continuous central coverage with gaps at the perimeter.
- The light yellow circles are buffers of radius one mile, the Oakland County standard. Employing the Oakland County standard provides a continuous block of coverage. As new areas come in to the city in 2007, as per boundary agreements, new sirens will need to be added to maintain coverage.
- The red outlines of polygons, in a sort of bubble foam, are outlines of the Dirichlet tesselation on the fire stations. The Dirichlet polygons are mutually exclusive and cover the entire area in the one mile buffer. Pick any point within the one mile buffer. Note which Dirichlet polygon contains it. Thus, the siren in the same Dirichlet polygon as the selected point is the siren closest to that selected point. Each Dirichlet polygon contains all the points closest to the siren in that polygon.

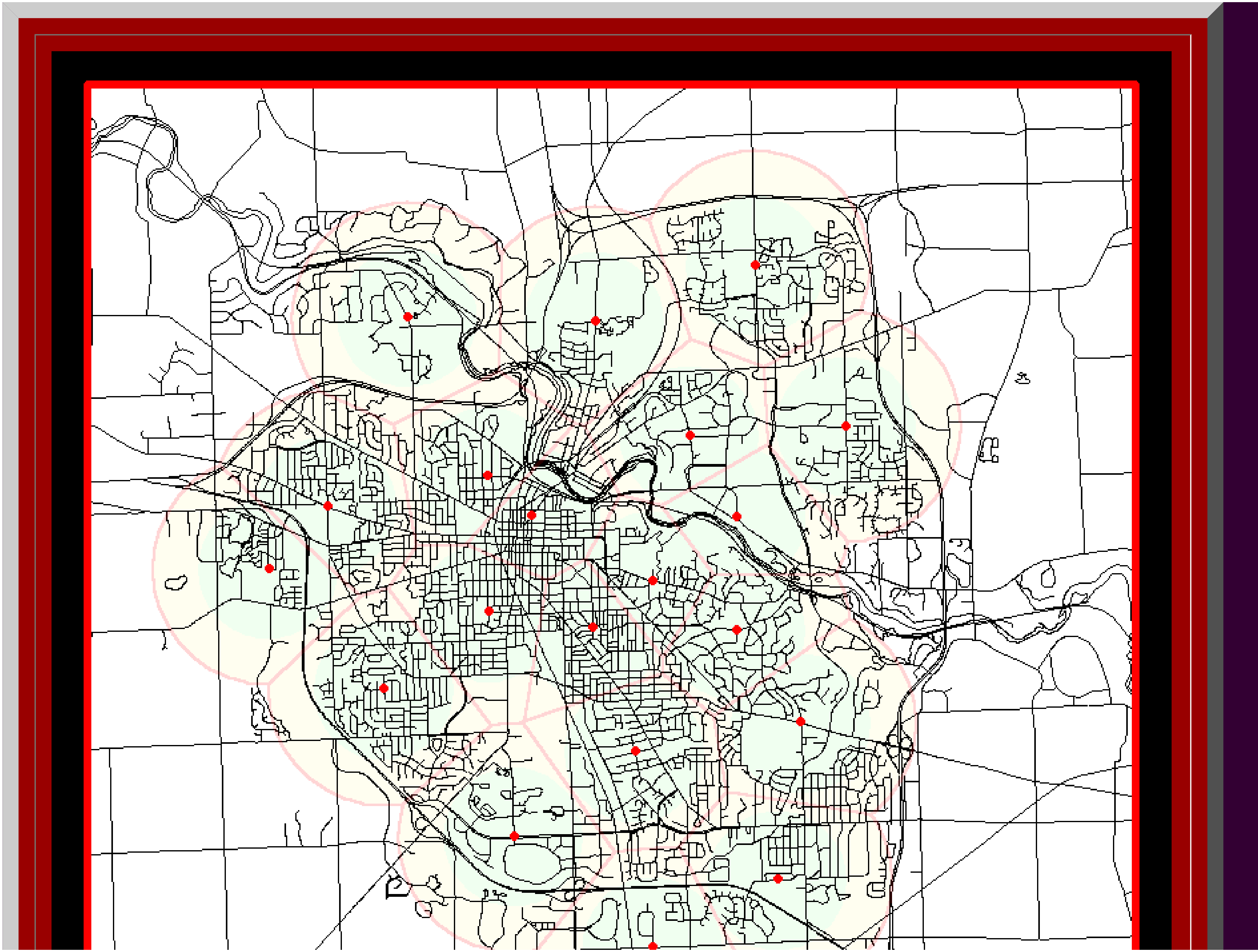

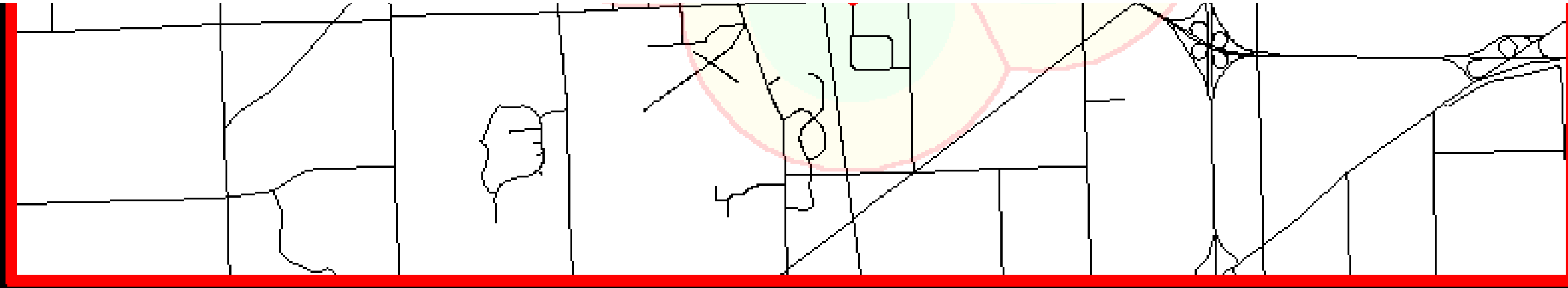

Figure 1. Red dots show existing tornado siren locations. Green circles use the coverage radius employed by Baltimore, MD; yellow circles use the coverage radius employed by Oakland County, MI.

In the second animated map, Figure 2,

- The red dots and the Dirichlet tesselation are as above.
- Successive buffers have radii of 1000, 2000, 3000, 4000, and 5000 feet.

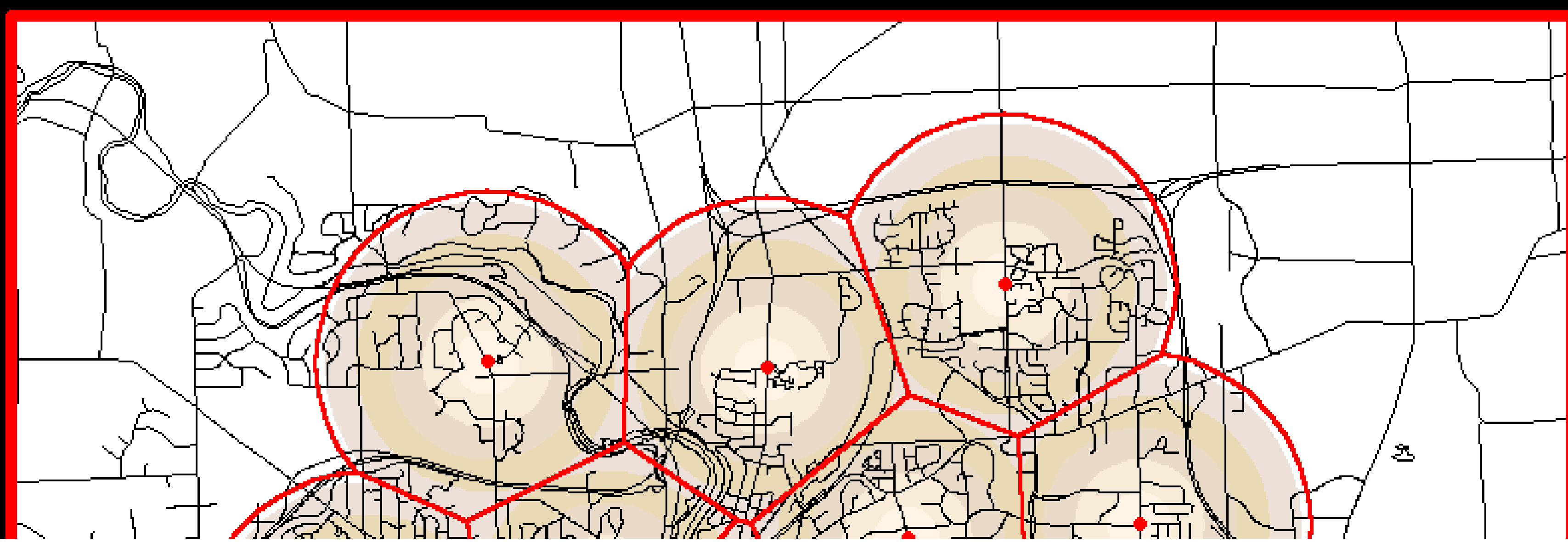

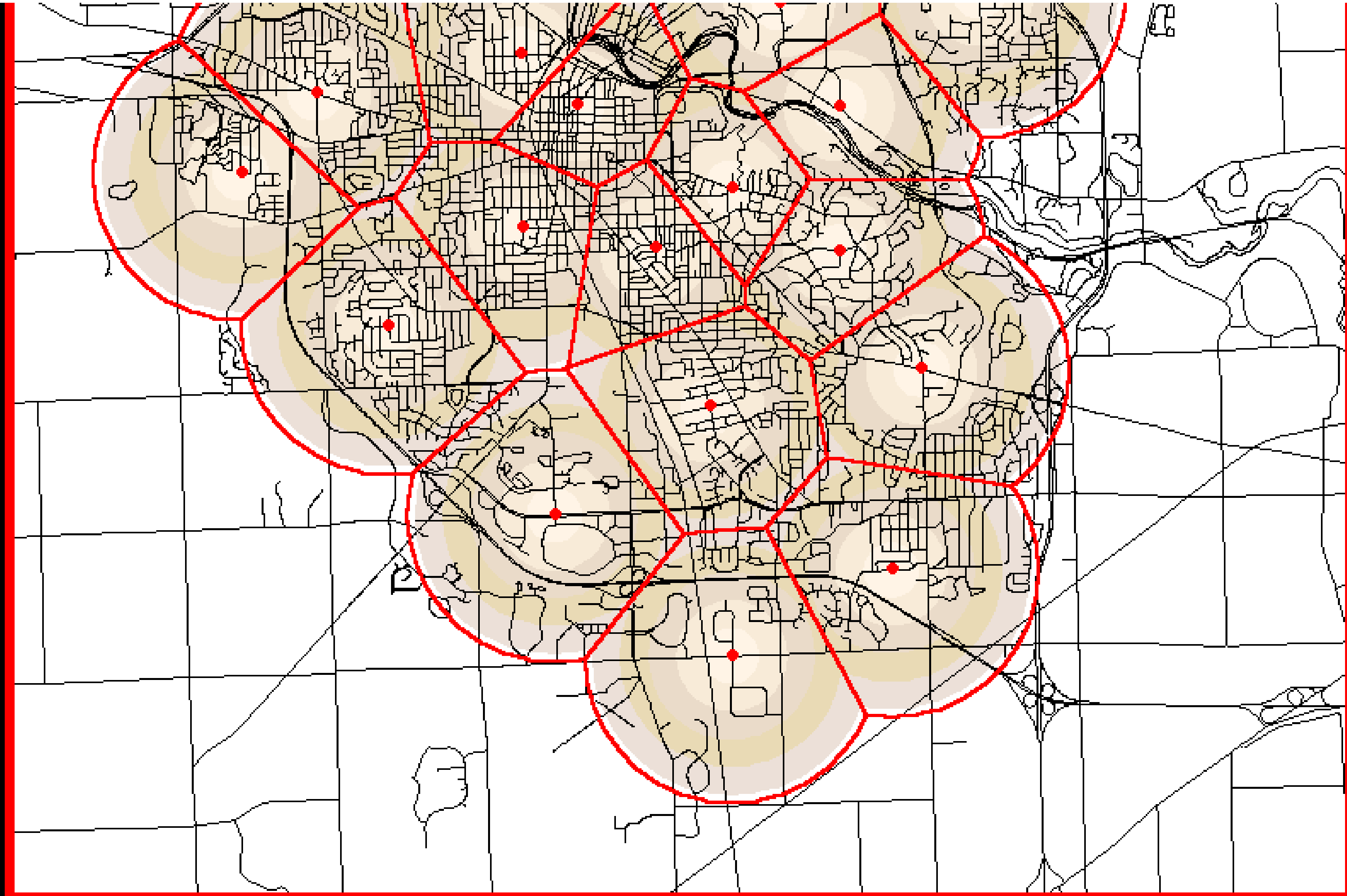

Figure 2. Spacing between successive buffers of sirens is 1000 feet.

In the third animated map, Figure 3,

- The red dots and the Dirichlet tesselation are as above. The white background has been removed, inverting the emphasis on the road network.

- Successive buffers have radii of 1000, 2000, 3000, 4000, and 5000 feet.
- Streets enter the picture along with buffers, showing zones of connectivity and perhaps suggesting emergency routes in the 3000 or 4000 foot buffer level. There is a northwest arterial that is entirely contained within the 4000 foot buffer. On the east side, routes through the southeast/central (Ann Arbor Hills) area show strong coverage.

Figure 3. In this view, connectivity of the road network, already within earshot of existing tornado sirens, is emphasized.

Finally, where might one consider locating new sirens (Figure 4)?

- The 5000 foot view shows a gap in coverage just south of Pioneer High School, east to the U. of M. golf course.
- Within the Dirichlet tesselation, highest priority might therefore (all other things being equal) be given to putting a siren in the gap; indeed, golfers are an important target population!
- Outside the Dirichlet tesselation, highest priority might therefore be given to the gap at the right edge of the tesselation that is within the freeway ring but is as yet uncovered by a siren. The location for a new siren was found by digitizing the uncovered area, calculating the centroid of the digitized region, and then using the centroid as the proposed siren location. In implementation, it is likely that actual position will not follow centroid location exactly as one factors in property rights, ease of siren maintenance/access, and so forth.

The cyan (turquoise) sets of concentric circles in Figure 4 fill these two gaps.

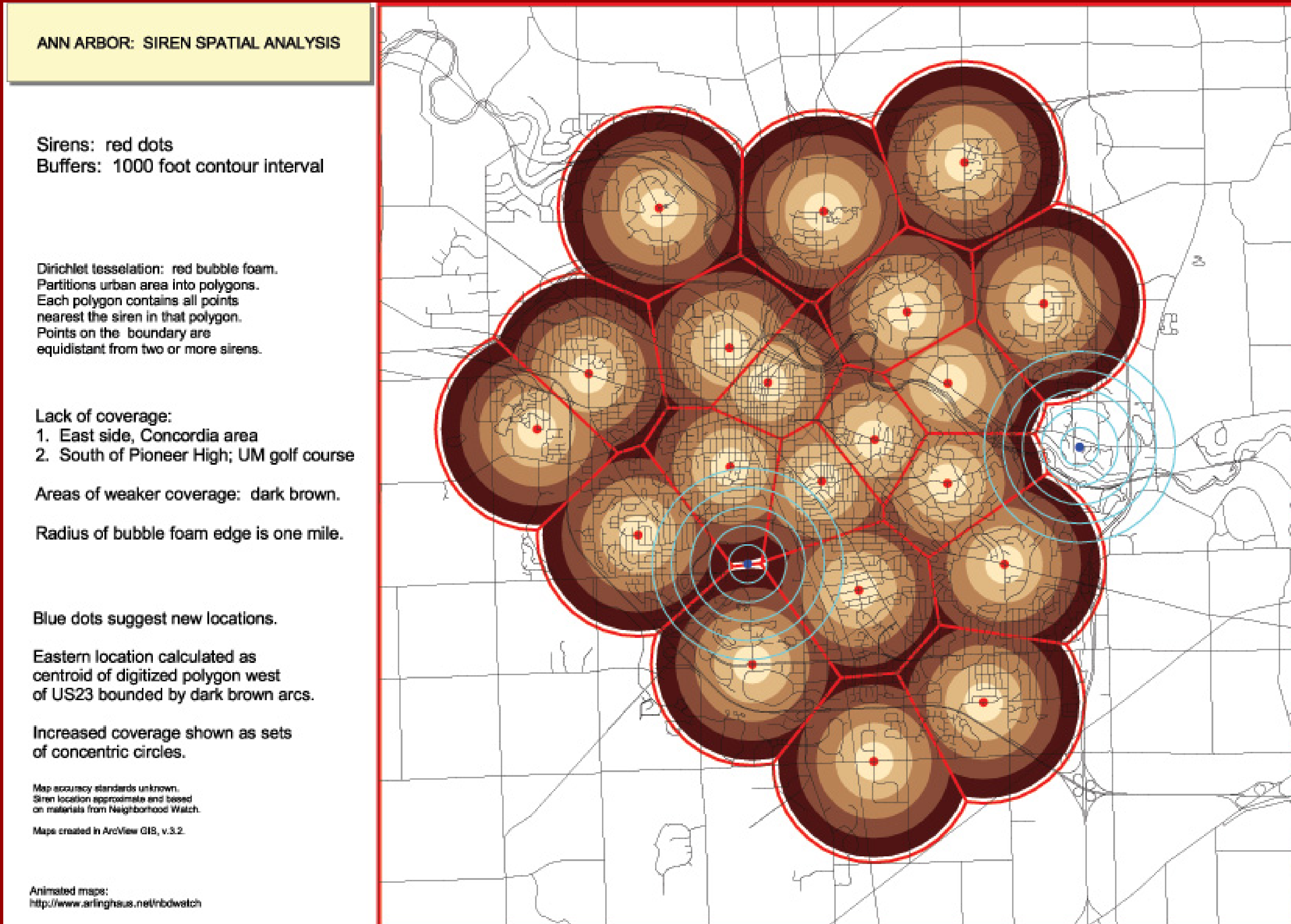

Figure 4. Cyan concentric circles targe locations for two new tornado sirens.

Click here for a link to an interactive map made using ImageMapper 3.1 from Alta4.com . Click on a dot on the linked map. Portions of the underlying database associated with that dot will pop up next to the map. The entries in the database are hypothetical and are present to suggest the range of power of this sort of map for organizing data. There is no need for any extra plug-in so that users who are NOT administrators of a machine may also have access to municipal files, from their local public library, public university, or elsewhere.

Directions for future research:

- Contour map of city
- Triangulated Irregular Network (TIN) made from contour map to show topography
- Superimposition of sirens on topographic map
- Recommendations for siren location or relocation based on this finer analysis.

Input from:

- Matthew Naud, Environmental Coordination Services, Director, City of Ann Arbor;
- Merle Johnson, Information Technology Services, City of Ann Arbor;

- Adele ElAyoubi, Neighborhood Watch Coordinator, City of Ann Arbor Police Department;
- Karen Hart, Planning Director, City of Ann Arbor.

Oakland County, Michigan
http://www.co.oakland.mi.us/ems/program_service/torn_siren.html

Baltimore, Maryland, Fire Department
http://www.ci.baltimore.md.us/government/fire/pr021016.html

Mail suggesting links of possible interest to Solstice readers

---

- **From Robert F. Austin: Interesting GIS page: http://www.geog.ubc.ca/courses/klink/g470/class00/gmenglan/frames.html**
- **From Ming-Hui Hsieh: software that allows us to split a picture, create a link for every mini-picture, and then put them back**

  together in a webpage. http://www.b-zone.de/software.htm
- **From Marc Schlossberg: Landsat images as art - http://astroboy.gsfc.nasa.gov/earthasart/**

Many thanks to Marc, Ming-Hui, and Bob for their thoughtfulness. Please feel free to communicate other links to Marc or Ming-Hui, or to IMaGe directly.

Educational Technology Experts:
Marc Schlossberg
Ming-Hui Hsieh
